Bistability between synchrony and incoherence in limit-cycle oscillators with coupling strength inhomogeneity

Tae-Wook Ko* and G. Bard Ermentrout†
Department of Mathematics, University of Pittsburgh, Pittsburgh, Pennsylvania 15260, USA
(Received 31 July 2007; revised manuscript received 21 February 2008; published 21 August 2008)

The effect of coupling strength inhomogeneity on the synchronization of identical oscillators is investigated. Through simulations and analysis of phase-reduced models, it is shown that the mean value of coupling function and the degree of inhomogeneity in the total of coupling strength to the each oscillator cooperate to stabilize incoherent states. Under some circumstances, there can be bistability between coherent and incoherent states. Various cases of coupled Morris-Lecar oscillators are studied as examples of our results.

DOI: 10.1103/PhysRevE.78.026210 PACS number(s): 05.45.Xt, 89.75.−k, 87.19.L−

I. INTRODUCTION

Synchronization of coupled oscillators is important and has been widely studied in a variety of systems from physics, chemistry, and biology [1–8]. The role of inhomogeneity has drawn attention from researchers in studies of synchronization and related topics including wave formation with the main focus on inhomogeneities in the intrinsic parameters of the oscillators, such as their uncoupled frequency. In addition to these inhomogeneities intrinsic to the oscillators themselves, many systems including neural systems [9,10] can have inhomogeneities in their coupling such as in coupling topology, coupling strength, and coupling type, and the effect of these inhomogeneities has begun to be explored [7,8,11–17].

Recently, several studies showed that inhomogeneity in coupling can affect the synchronization of coupled oscillators [11–15]. Golomb and Hansel studied the effect of inhomogeneity of the number of inputs to oscillators in randomly coupled oscillators with uniform coupling strength using the phase reduction method [11]. They found that the system synchronizes above a critical number of inputs, in which case the inhomogeneity of the number of inputs becomes small enough not to interfere with the synchronization [11]. After the introduction of the concept of a "scale-free network," which has a very broad distribution in the number of connections per element [18], Nishikawa *et al.* studied the synchronization of coupled oscillators with uniform coupling strength on this type of network. They showed that synchronization is much harder to achieve in the networks with strong inhomogeneity in the number of inputs than in random homogeneous networks [12]. In later papers, it was also shown that when the coupling strength is weighted by the inverse of the number of inputs, synchronization is enhanced [13,14]. Denker *et al.* studied the effect of coupling strength inhomogeneity in networks of pulse-coupled oscillators with directed random connectivity and found that the coupling strength inhomogeneity leads to asynchronous, aperiodic states [15].

In this paper, we study the effects of coupling strength inhomogeneity on synchronization in phase-reduced models by explicitly introducing the inhomogeneity. Understanding the effects in phase-reduced models is useful, since such models can represent many aspects of coupled limit-cycle oscillators. For example, they can be a model for synaptically or electrically coupled Morris-Lecar oscillators [19,20] or FitzHugh-Nagumo oscillators [21]. We show that incoherent states can be stabilized as we increase the inhomogeneity of the coupling strength. Surprisingly, we find that the system can exhibit bistability between a coherent state and an incoherent state, which does not exist in the systems with homogeneous coupling strengths. Using a Fokker-Planck equation for the population density of oscillators, we show how the coupling function plays a role in determining the critical amount of inhomogeneity required for a stable incoherent state.

II. MORRIS-LECAR OSCILLATORS WITH COUPLING STRENGTH INHOMOGENEITY

As an example of coupled limit-cycle oscillators with coupling strength inhomogeneity, we study Morris-Lecar (ML) oscillators with synaptic or electric coupling [19,20]:

$$C\frac{dV_i}{dt} = -I_{l,i} - I_{\mathrm{K},i} - I_{\mathrm{Ca},i} - I_{c,i} + I$$
$$= -\bar{g}_l(V_i - E_l) - \bar{g}_{\mathrm{K}} w_i (V_i - E_{\mathrm{K}})$$
$$- \bar{g}_{\mathrm{Ca}} m_\infty(V_i)(V_i - E_{\mathrm{Ca}}) - I_{c,i} + I,$$

$$\frac{dw_i}{dt} = \phi\frac{[w_\infty(V_i) - w_i]}{\tau_w(V_i)}, \qquad i = 1,2,\ldots,N, \qquad (1)$$

where $I_{c,i}$ is the coupling current to oscillator i, I (in $\mu\mathrm{A/cm}^2$) is an injected current, and N is the total number of oscillators. Details of the functions and the parameter values are in Appendix A. With these parameter values, the uncoupled single ML oscillator shows monostable periodic firing for I between $I_1=40$ and $I_2=98$. The periodic firing appears via a saddle-node on invariant circle bifurcation and thus the frequency of the firing can be arbitrarily small near the bifurcation point [20,22].

We simplify the coupling as a mean field weighted by K_i. The dependence of K_i on i reflects the inhomogeneity in the total coupling strength to the oscillators. For synaptic cou-

*taewook@pitt.edu
†bard@math.pitt.edu

pling, the coupling current $I_{c,i}$ is $I_{syn,i}$ given by

$$I_{syn,i} = \frac{K_i}{N}\sum_{j=1}^{N} s_j(V_i - E_{syn}), \tag{2}$$

where s_j is a synaptic gating variable. The kinetics of s_j and the value of E_{syn} are described in Appendix A. With the given value of E_{syn}, the synaptic coupling is excitatory. For gap junction coupling, the coupling current $I_{c,i}$ is $I_{gap,i}$ given by

$$I_{gap,i} = \frac{K_i}{N}\sum_{j=1}^{N} (V_i - V_j). \tag{3}$$

In Eqs. (2) and (3), the coupling strengths K_i are randomly assigned from $K_0[1-\Delta K, 1+\Delta K]$, where $\Delta K \in [0,1]$ and we use $K_0=0.1$ so that the couplings are weak enough not to distort the limit cycle significantly. For weak coupling, we can apply phase-reduction method to this model. In cases without noise, K_0 does not affect phase distribution of the system as long as K_0 is small.

We simulate the full model for different injected currents: $I=45$, 50, and 80. For these injected currents, a single uncoupled oscillator shows a periodic oscillation. Among the three injected currents, smaller I is closer to the saddle node bifurcation point.

We use two kinds of initial conditions: (i) near-synchronous states where the oscillators initially lie on almost the same points on the limit cycle or (ii) near-incoherent states where the oscillators almost uniformly distributed over the period of the oscillators. We simulate Eq. (1) using a fourth-order Runge-Kutta method with time step $\Delta t=0.01$.

Figure 1 shows the raster plots for synaptically coupled cases for $I=50$ and $I=80$. Results with $I=45$ are similar to those with $I=50$ (not shown). Every time an oscillator spikes, a dot is plotted at the time-oscillator index point. The system shows highly synchronous behaviors for both of the injection currents with small amount of coupling strength inhomogeneity [Fig. 1(a) for $I=50$ and Fig. 1(d) for $I=80$]. However, the system shows different behaviors for larger inhomogeneity. While the system still exhibits highly synchronous states for $I=80$ [Fig. 1(e)], it shows bistability between synchronous and incoherent states for $I=50$ [Figs. 1(b) and 1(c)]. With gap junction coupling, the system shows only synchronous states for all the injection currents and the inhomogeneity considered (not shown). Phase-reduced systems from Eq. (1) [3–6] show similar behaviors.

In subsequent sections, we show that the shape of the phase-reduced interaction function plays a critical role in determining the stability of the synchronous and incoherent states. As the shape of the functions depends on both the firing rate and the nature of the coupling, we are able to explain the results of Fig. 1.

III. PHASE MODEL AND SIMULATIONS

We use phase-reduced models to understand the effect of coupling strength inhomogeneity. We study identical coupled

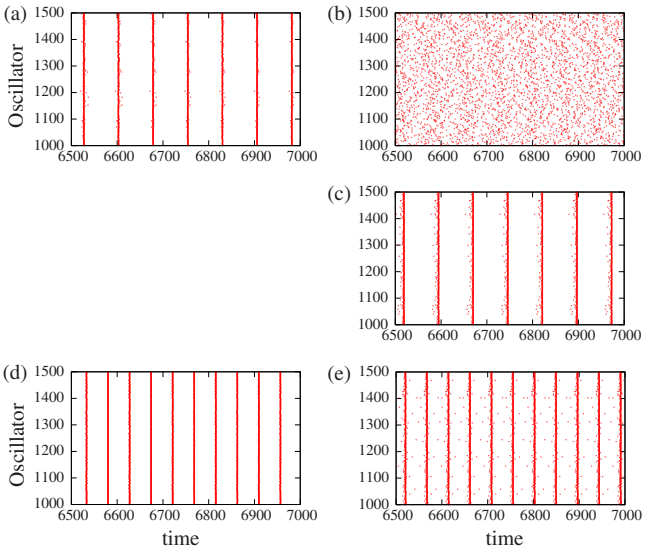

FIG. 1. (Color online) Raster plots for ML oscillators with different degrees of the coupling strength inhomogeneity. The oscillators are synaptically coupled. $N=3200$ and $K_0=0.1$. Near-synchronous initial conditions (SICs) or near-incoherent initial conditions (IICs) are used. $I=50$: (a) $\Delta K=0.5$ and IIC, (b) $\Delta K=1.0$ and IIC, (c) $\Delta K=1.0$ and SIC. $I=80$: (d) $\Delta K=0.5$ and IIC, (e) $\Delta K=1.0$ and IIC.

oscillators with same type of coupling as this is the simplest case which clearly illustrates the coupling strength inhomogeneity effect. Systems of weakly coupled identical limit-cycle oscillators can be reduced to the following system [3–6]:

$$\dot{\theta}_i(t) = \omega + \frac{1}{N}\sum_{j=1}^{N} K_{ij}H(\theta_j(t) - \theta_i(t)) + \sqrt{2D}\xi_i(t),$$

$$i = 1,2,\ldots,N, \tag{4}$$

where $\theta_i(t)$ is the phase of ith oscillator at time t, ω is the natural frequency of the oscillators, and N is the total number of oscillators. The second term on the right side denotes the coupling between oscillator i and other oscillators. K_{ij} is the coupling strength from oscillator j to oscillator i and $K_{ij} \geqslant 0$. $H(\theta)$ is the coupling function obtained by the phase reduction method for pairwise interaction [3–6]. $H(\theta)$ is a 2π-periodic function and depends only on the phase difference of the interacting oscillators. In general, the coupling function $H(\theta)$ can be written as a Fourier series:

$$H(\theta) = c_0 + \sum_{m=1} c_m \sin(m\theta + \beta_m), \quad c_m \geqslant 0,$$

$$m = 1,2,\ldots \ . \tag{5}$$

The third term of Eq. (4) is the noise. $D \geqslant 0$ is the noise strength and $\xi_i(t)$ are independent white noise processes having the properties

$$\langle \xi_i(t) \rangle = 0, \quad \langle \xi_i(t)\xi_j(t') \rangle = \delta_{ij}\delta(t-t'). \tag{6}$$

In the absence of the noise term, the requirement for the system to have a perfectly synchronous state is that the coupling term be the same for all the oscillators when they have the same phase. This is satisfied in two different ways: condition (a) $H(0)=0$; condition (b) $S_i \equiv \frac{1}{N}\Sigma_{j=1}^{N} K_{ij}$ is the same for all i. These conditions can be satisfied independently. When one of these condition is satisfied and each oscillator is directly or indirectly influenced by every other oscillator through the connection networks, the local stability condition for the synchronous state is $H'(0)>0$ [23]. In this paper, we study the case where condition (b) is not satisfied. We require $H'(0)>0$ to be satisfied so that synchronous states are stable without the inhomogeneity in S_i and noise.

In the studies with homogeneous coupling strength sum S_i, c_0 in Eq. (5) has no effect on the dynamics of the system except changing the frequency uniformly and thus has been usually ignored or introduced to match frequencies. However, when the coupling has some spatial inhomogeneity as in the case of a linear chain of nearest coupled oscillators where oscillators at the boundaries have different coupling, c_0 can contribute to the inhomogeneity of frequencies and thus the nontrivial dynamics of the system [24]. Similarly, in randomly coupled oscillator cases where the number of inputs is not homogeneous, it was shown that c_0 can cause desynchronization by contributing to the effective frequency distribution [11]. Thus, we can expect desynchronization due to both c_0 and the inhomogeneity in S_i in our system. Note that the violation of condition (b) does not necessarily mean the absence or destabilization of perfectly synchronous states or coherent states [e.g., if condition (a) holds]. Further, we note that for gap junction coupling, $H(0)=0$ [25]. Thus, as long as $H'(0)>0$, synchrony is always stable.

We mainly study the simplest case of inhomogeneous coupling $K_{ij}=K_i$, where K_i is chosen randomly from $[1-\Delta K, 1+\Delta K]$. This interval is general in the sense that cases with other intervals can be transformed to cases with this one. We thus focus on

$$\dot{\theta}_i(t) = \omega + \frac{K_i}{N}\sum_{j=1}^{N} H(\theta_j(t)-\theta_i(t)) + \sqrt{2D}\xi_i(t),$$

$$i = 1,2,\ldots,N. \tag{7}$$

This model is the simplest generalization of the thoroughly studied model for globally coupled oscillators with $K_i=K$ [3–5], so it is easy to analyze and simulate. In this model, $S_i=K_i$ and thus the inhomogeneity of K_i corresponds to the inhomogeneity of S_i. As shown numerically at the end of this section, this model can be a good approximation of the general model of Eq. (4) when $\frac{1}{N}\Sigma_{j=1}^{N} K_{ij}=K_i$ and oscillators are randomly coupled. This model can be considered as a mean-field approximation of general cases.

We see that in this model c_0 can have a desynchronizing effect in relation with the harmonic part $H_h(\theta) \equiv \{H(\theta)-c_0\}$ [11]. In the extreme case in which $|c_0|$ is much greater than $|H_h(\theta)|$ for all θ, the system can have effective frequency differences in the presence of the inhomogeneity and thus can show incoherent behaviors. However, in the cases with $|c_0|$ and $|H_h(\theta)|$ in the same range, it is not obvious that stable incoherent behavior exists. Here, we mainly consider c_0 as a parameter of the coupling function and study the family of coupling functions $c_0+H_h(\theta)$ for a given $H_h(\theta)$ of a coupling function $H(\theta)$.

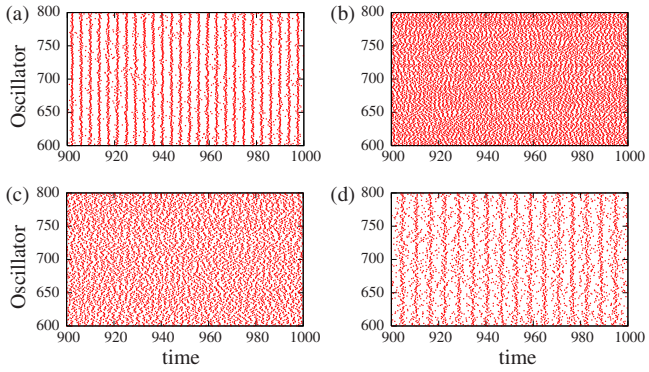

FIG. 2. (Color online) Raster plots showing the effect of the coupling strength inhomogeneity and c_0 of Eq. (8). $D=0.1$. K_i is randomly selected from $[1-\Delta K, 1+\Delta K]$. $\beta_1=-0.3\pi$. $N=1600$. (a) $\Delta K=0.4$, $c_0=0.7$. (b) $\Delta K=0.4$, $c_0=1.8$. (c) $\Delta K=1.0$, $c_0=0.7$. (d) $\Delta K=1.0$, $c_0=0$. Random initial condition from $[0,2\pi)$ is used.

Let us first consider the case with $H(\theta)=c_0+\sin(\theta+\beta_1)$, where $\beta_1 \in (-\pi/2, \pi/2)$. This coupling function is a good approximation of many general coupling functions and satisfies the condition $H'(0)>0$. Equation (7) becomes

$$\dot{\theta}_i = \omega + \frac{K_i}{N}\sum_{j=1}^{N}[c_0 + \sin(\theta_j - \theta_i + \beta_1)] + \sqrt{2D}\xi_i(t)$$

$$= \omega + K_i[c_0 + R_1 \sin(\Theta_1 - \theta_i + \beta_1)] + \sqrt{2D}\xi_i(t), \tag{8}$$

where R_n and Θ_n are the order parameters and corresponding phases, respectively, defined by

$$R_n e^{in\Theta_n} = \frac{1}{N}\sum_{j=1}^{N} e^{in\theta_j}, \quad n = 1,2,\ldots. \tag{9}$$

It was shown that almost all initial conditions lead to the synchronous state in cases with $K_i=K$ and $D=0$ [26,27].

We simulate Eq. (8) using the Euler method with time step $\Delta t=0.01$. A smaller time step does not significantly alter the results. We use two kinds of initial conditions: (i) $\theta_i(0)$ chosen randomly from $[0,2\pi)$ or (ii) $\theta_i(0)=\epsilon_i$, where ϵ_i is a random number chosen from $[0,\delta]$ with δ small.

Figures 2(a)–2(d) are raster plots showing the effect of coupling strength inhomogeneity and the constant c_0 of the coupling function. Every time an oscillator reaches phase 2π, a dot is plotted at the time-oscillator index point. Even though the coupling strength inhomogeneity is the same for Figs. 2(a) and 2(b), the system shows totally different behaviors with different c_0. The system can show coherent behavior with small c_0 [Fig. 2(a)], but incoherent behavior with c_0 beyond some critical value [Fig. 2(b)]. We can observe similar transition from coherent states to incoherent states if we increase the inhomogeneity with other parameters fixed [Figs. 2(a)–2(c)]. Figure 2(c) with increased ΔK shows inco-

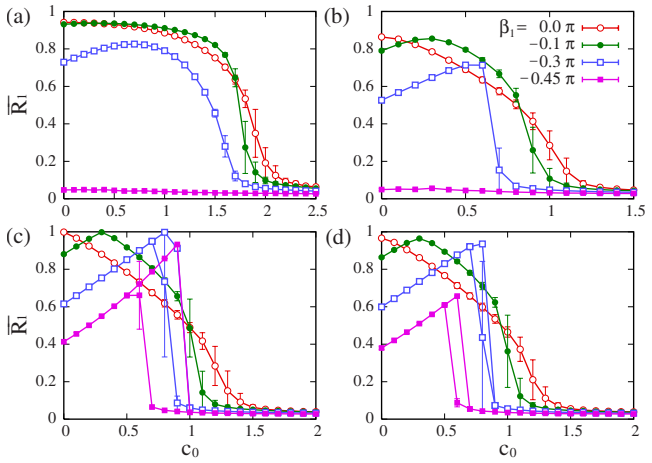

FIG. 3. (Color online) Averaged order parameter $\overline{R_1}$ versus c_0 for Eq. (8) with different values of β_1. (a) $D=0.1$ and $\Delta K=0.4$. (b) $D=0.1$ and $\Delta K=1.0$. (c) $D=0$ and $\Delta K=1.0$. (d) $D=0.02$ and $\Delta K=1.0$. The symbols represent the averaged order parameters which are obtained by first averaging order parameter R_1 of Eq. (9) over time and then over simulations with different $\{K_i\}$ and noise configurations. For more detail, see the text. The error bars indicate the standard deviation of the time-averaged order parameters and the curves are guides for the eyes. $N=1600$.

herent behavior compared to (a). If we decrease c_0 in the case of Fig. 2(c), we can get more coherent behavior [Fig. 2(d)]. These raster plots show that coupling strength inhomogeneity and c_0 of coupling function can cause the desynchronization of the system.

To see how the dynamics of the system depends on c_0, β_1, and ΔK, we measure the order parameter. For each point of Fig. 3, we simulate with ten different configurations of the system. More specifically, we use ten different sets of K_i and noise. From the initial conditions, the system evolves to a steady state. The order parameter R_1 approaches a value with small fluctuation and the fluctuation decreases as we increases the total number of oscillators. Thus, we conclude that the fluctuation is due to finite-size effects, and in the limit of infinite size, the system approaches a steady state characterized by a single order parameter. We calculate the time average of the order parameter for each simulation after transient states. Then, the time-averaged order parameters are averaged over the simulations with the same kind of initial conditions, creating two ensemble averages for the two different initial conditions, respectively. We plot both of them if the two ensemble averages are significantly different, otherwise we plot one of them. In Fig. 3(a) with coupling strength inhomogeneity ($\Delta K=0.4$) and noise ($D=0.1$), the system exhibits coherent states when c_0 is small, but shows incoherent states beyond some critical c_0 value which depends on β_1 and ΔK. The critical c_0 value usually decreases as $|\beta_1|$ or ΔK increases. Except for $\beta_1=-0.45\pi$, the curves have peak near $c_0=-\sin\beta_1$ (>0) which makes $H(0)=0$. For $\beta_1=-0.45\pi$, the system shows incoherent behavior for all c_0. Figure 3(b) shows similar behavior with a larger coupling strength inhomogeneity ($\Delta K=1.0$). The critical c_0 values become smaller and the order parameter values are also smaller compared to those of Fig. 3(a). In Fig. 3(c), without noise ($D=0$), which is one of the sources of disorder in the system, we can still see the transition from coherent to incoherent states. The system shows perfectly synchronous states with $c_0=-\sin\beta_1$. The states with order parameters less than one but significantly greater than 0 are partially locked states in these cases without noise. The critical c_0 values become larger compared to those of Fig. 3(b) with the same amount of inhomogeneity ($\Delta K=1.0$). Now we can see the coherent-incoherent transition for $\beta_1=-0.45\pi$. This is because the incoherent state is stable for $\beta_1=-0.45\pi$ even with $c_0=0$ for noisy cases of Figs. 3(a) and 3(b), but unstable in this case without noise. Note that there exists bistability between coherent and incoherent states for β_1 near $-\pi/2$ and c_0 near $-\sin\beta_1$. In the bistable region, the system reaches either an incoherent state or a coherent state depending on the initial conditions. The former is obtained with near incoherent initial conditions and the latter is with near perfectly synchronous initial conditions. We can still see the bistability in the presence of small amount of noise, but the bistable region becomes smaller for larger noise [Fig. 3(d)].

The mechanism for this bistability between coherent and incoherent states differs from those of previous studies, where the bistability is due to time-delayed interaction [28,29] or the dynamic change of coupling strengths [17] or strong coupling [11]. The bistability of our model is caused by the desynchronization due to the coupling strength inhomogeneity near the parameter range where coherent states are locally stable. Our mechanism implies that the bistability can occur in randomly and sparsely coupled oscillators where a nonuniform number of inputs effectively introduces a coupling strength inhomogeneity [11]. This phenomenon may be related to the recently reported bistability between synchronous states and chimera states in nonlocally coupled identical oscillators [30–32]. In chimera states, phase-locked oscillators coexist with drifting ones. Similar to the bistability of our model, the bistability between a synchronous state and a chimera state was shown to occur for the same coupling function of Eq. (8) when β_1 is near $-\pi/2$ [30–32].

Simulations with more general coupling functions with a dominant mth-order term in Eq. (5) show a similar transition from coherent states to incoherent states. In these simulations, the order parameter R_m defined by Eq. (9) exhibits the transition as c_0 changes.

Even though the model Eq. (7) is simple and idealized, it is a good approximation of more complex situations. In Fig. 4, we compare the results from Eq. (8) and those from the following randomly coupled oscillator model with $H(\theta)=c_0+\sin(\theta+\beta_1)$ and sufficiently large number of connections:

$$\dot{\theta}_i = \omega + \frac{K_i}{\sum_{j=1}^{N} w_{ij}} \sum_{j=1}^{N} w_{ij} H(\theta_j(t) - \theta_i(t)) + \sqrt{2D}\xi_i(t), \tag{10}$$

where w_{ij} is introduced to implement the inhomogeneity in all the coupling strengths in addition to the inhomogeneity in coupling strength sum. In this coupled oscillator model, the connections between oscillators are given by bidirectional random network where two oscillators have connection with a constant probability and the connection is bidirectional [8].

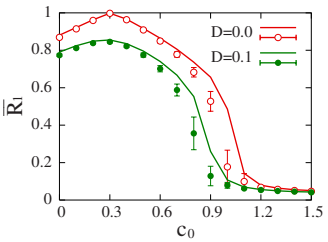

FIG. 4. (Color online) Averaged order parameter $\overline{R_1}$ versus c_0 for randomly coupled oscillators of Eq. (10). The symbols represent the averaged order parameters which are obtained by first averaging order parameter R_1 of Eq. (9) over time and then over simulations with different $\{w_{ij}\}$, networks, and noise configurations. The error bars indicate the standard deviation of the time-averaged order parameters. The curves are those connecting averaged order parameters for the same parameters in Figs. 3(b) and 3(c) for the all-to-all coupling case. $N=1600$, $\Delta K=1.0$, average number of neighboring oscillators $\bar{k}=20$, and $\beta_1=-0.1\pi$.

w_{ij} is nonzero only for connected oscillators and randomly selected from [0,2]. This range is chosen because it gives the worst case among the distribution in the form of $[1-\Delta w, 1+\Delta w]$ with $\Delta w \in [0,1]$. Without the multiplication by $K_i/\Sigma_{j=1}^{N} w_{ij}$, the system shows coherent behavior. This is due to the fact that the sums $\Sigma_{j=1}^{N} w_{ij}$ are distributed closely to the average value for a large enough number of neighboring oscillators. By dividing the interaction sum by $\Sigma_{j=1}^{N} w_{ij}$, we can control the inhomogeneity of coupling strength sum through K_i only and can see its effect. We simulate with ten different $\{w_{ij}\}$, networks, and noise configuration and calculate the averaged order parameters. Figure 4 shows the averaged order parameter $\overline{R_1}$ as a function of c_0. The curves from Fig. 3 of the all-to-all coupling case fit well with those values. This indicates that the globally coupled model with the inhomogeneity only in K_i is a good approximation of randomly coupled oscillator model of Eq. (10) as far as the incoherence-coherence transition is concerned.

Note that the randomly coupled oscillator model has a stable in-phase state synchronous state when $H(0)=0$ and $H'(0)>0$ (theorem 3.1 of Ref. [23]) and shows incoherent states as the globally coupled model. Therefore, we can observe at least the bistability between an incoherent state and an in-phase state in this model. However, the nonuniformity in w_{ij} and the sparseness of the connections act as sources of disorder and thus can affect the coherent states other than in-phase states. We see that the coherent states observed in the mean-field model with $c_0 > c_0^*$ disappear first for larger c_0 as Δw increases and/or the average number of connections decreases.

IV. ANALYSIS OF THE POPULATION DENSITY EQUATION

We can analyze the transition from uniformly incoherent states to coherent states of Eq. (7) using standard population density analysis [4,5,11,33,34]. As $N\to\infty$, we can define a density $\rho(\theta,K,t)$ for each K such that $\rho(\theta,K,t)d\theta$ denotes the fraction of oscillators whose phase lies between θ and $\theta+d\theta$, where K corresponds to K_i. The density $\rho(\theta,K,t)$ should satisfy the Fokker-Planck equation [4,5,11,33,34]

$$\frac{\partial \rho(\theta,K,t)}{\partial t} = -\frac{\partial\{\rho(\theta,K,t)v\}}{\partial\theta} + D\frac{\partial^2\rho(\theta,K,t)}{\partial\theta^2}$$
$$= -\frac{\partial}{\partial\theta}\left\{\rho(\theta,K,t)\left[\omega + K\int_0^\infty\int_0^{2\pi} \times H(\theta'-\theta)\rho(\theta',K',t)g(K')d\theta'\,dK'\right]\right\} + D\frac{\partial^2\rho(\theta,K,t)}{\partial\theta^2}, \quad (11)$$

where $g(K)$ is the probability density for K.

The uniformly incoherent state with $\rho(\theta,K,t)=1/2\pi$ is a solution of Eq. (11). To find the transition point between coherent states and the uniformly incoherent state, we do a linear analysis around the uniformly incoherent state and obtain the following equations for the eigenvalue $\lambda_n=\mu_n-i\Omega_n-in\omega$ which determines the stability of mode n with n being an integer. Here, we use the Fourier series of the coupling function $H(\theta)$ [Eq. (5)]. We consider only cases with $c_0\geq 0$, since cases with $c_0<0$ can be transformed to these cases:

$$\frac{2\cos\beta_n}{nc_n} = \int_0^\infty \frac{Kg(K)(\mu_n+n^2D)dK}{(\mu_n+n^2D)^2+(nKc_0-\Omega_n)^2}, \quad (12)$$

$$\frac{2\sin\beta_n}{nc_n} = \int_0^\infty \frac{-Kg(K)(nKc_0-\Omega_n)dK}{(\mu_n+n^2D)^2+(nKc_0-\Omega_n)^2}. \quad (13)$$

These equations are similar to those obtained in Ref. [11]. In Ref. [11], the effect of the inhomogeneity of the number of inputs to oscillators was studied, and the number of inputs was used instead of K of our system to derive those equations.

In this paper, we deal with the simple case with $g(K)=1/(2\Delta K)$ for $K\in[1-\Delta K,1+\Delta K]$ and $g(K)=0$ otherwise. In this case, Eqs. (12) and (13) become

$$\frac{\cos\beta_n}{nc_n} = \frac{1}{4\Delta K}\int_{1-\Delta K}^{1+\Delta K} \frac{K(\mu_n+n^2D)dK}{(\mu_n+n^2D)^2+(nKc_0-\Omega_n)^2}, \quad (14)$$

$$\frac{\sin\beta_n}{nc_n} = \frac{1}{4\Delta K}\int_{1-\Delta K}^{1+\Delta K} \frac{-K(nKc_0-\Omega_n)dK}{(\mu_n+n^2D)^2+(nKc_0-\Omega_n)^2}. \quad (15)$$

Writing $D'\equiv\frac{nD}{c_n}$, $c_0'\equiv\frac{c_0}{c_n}$, $\mu_n'\equiv\frac{\mu_n}{nc_n}$, and $\Omega_n'\equiv\frac{\Omega_n}{nc_n}$, we can rewrite Eqs. (14) and (15):

$$\cos\beta_n = \frac{1}{4\Delta K}\int_{1-\Delta K}^{1+\Delta K} \frac{K(\mu_n'+D')dK}{(\mu_n'+D')^2+(Kc_0'-\Omega_n')^2}, \quad (16)$$

$$\sin\beta_n = \frac{1}{4\Delta K}\int_{1-\Delta K}^{1+\Delta K} \frac{-K(Kc_0'-\Omega_n')dK}{(\mu_n'+D')^2+(Kc_0'-\Omega_n')^2}. \quad (17)$$

When $\cos\beta_n<0$—in other words, $\beta_n\in(\pi/2,\pi]\cup(-\pi,-\pi/2)$—the left-hand side of Eq. (14) is always negative and thus μ_n, the real part of λ_n, should be

negative to satisfy the equality. Therefore, in this case, the corresponding eigenmode decays regardless of coupling strength inhomogeneity. To avoid the case of trivially stable incoherent state, we require that at least one β_n is outside of those range. Note that if $\beta_n \in (\pi/2, \pi] \cup (-\pi, -\pi/2)$ for all n then $H'(0) < 0$ which violates our assumption of stable synchrony for homogeneous coupling strength cases. Therefore, we consider modes with $\beta_n \in (-\pi/2, \pi/2)$ in the following analysis.

Before discussing general cases, let us consider the case with $c_0=0$. From Eqs. (14) and (15), we obtain the following expression of λ_n for the uniform distribution $g(K)$:

$$\lambda_n = \left(\frac{n}{2} c_n \cos\beta_n - n^2 D\right) - in\left(\frac{c_n}{2}\sin\beta_n + \omega\right). \quad (18)$$

This shows that in this case the stability is independent of the width ΔK of coupling strength inhomogeneity. We numerically find that $\mathrm{Re}(\lambda_n)$ decreases monotonically as c_0 or ΔK increases when $c_0 \neq 0$. An increase in c_0 or ΔK stabilizes the incoherent state. Therefore, if $\mathrm{Re}(\lambda_n) < 0$ for all n when $c_0 = 0$, the incoherent state is stable regardless of c_0. This is the case for the cases with $\beta_1 = -0.45\pi$ and $D=0.1$ of Figs. 3(a) and 3(b). As we change c_0, the system can show the transition from coherent states to incoherent states where $\mathrm{Re}(\lambda_n) < 0$ for all n only when $\frac{n}{2} c_n \cos\beta_n > n^2 D$ for at least one n.

For each mode number n, we can find the critical c_0 above which the corresponding mode decays. Let us call it c_{0n}^*. The critical c_0, c_0^*, above which the uniformly incoherent state become stable is given by

$$c_0^* = \max_n \{c_{0n}^*\}. \quad (19)$$

As mentioned above, we numerically observe that the real part of the eigenvalue, μ_n', decreases monotonically from the maximum value $(\frac{1}{2}\cos\beta_n - D')$ as we increase c_0' or ΔK with other parameters fixed. From the Eqs. (16) and (17) with fixed ΔK and β_n, we can see that as D' increases, the same set of c_0' and Ω' is a solution for the same value of $\mu_n' + D'$. Therefore when D' changes from D' to $D' + \Delta D'$, μ_n' decreases by $\Delta D'$ for the same c_0' and thus the curve for μ_n' versus c_0' moves downward by $\Delta D'$. The critical c_0' for which $\mu_n' = 0$ decreases with the increase of D'. We also observe that β_n does not significantly affect the order magnitude of c_{0n}^*. For general coupling function $H(\theta)$, c_n is usually smaller for larger n, so the effective noise $D'(=nD/c_n)$ is larger for fixed D and ΔK. Thus, the critical c_0' is smaller for larger n and c_{0n}^* is much smaller, because $c_0 = c_0' c_n$. Therefore, c_0^* is usually determined by the lower order harmonics of $H(\theta)$.

To find out the critical c_0 for the cases with noise ($D > 0$), we numerically find c_0', μ_n', and Ω_n' that satisfy Eqs. (16) and (17). The critical c_0' is obtained with $\mu_n' = 0$. The system shows a Hopf bifurcation from incoherent states to coherent states as c_0 decreases. It is a Hopf bifurcation since the imaginary part of the eigenvalue corresponding to $\mu_n' = 0$ is not zero. The system exhibits n-cluster states when the mode n destabilizes.

For the cases without noise [$D'=0$ in Eqs. (16) and (17)], we consider the limit of $\mu_n' \to 0^+$ for each n to find the critical c_0 [4,33]. In this limit, if $(Kc_0' - \Omega_n')$ vanishes for some K in the integration range, the right-hand side of Eq. (16) can have a value other than zero and there can be c_0' satisfying this equation. More specifically, the condition is that $c_0'(1 - \Delta K) - \Omega_n' < 0$ and $c_0'(1 + \Delta K) - \Omega_n' > 0$ for a positive c_0'. We integrate the right-hand sides of Eqs. (16) and (17), and obtain

$$\cos\beta_n = \frac{\Omega_n' \pi}{4 c_0'^2 \Delta K}, \quad (20)$$

$$\sin\beta_n = \frac{-4c_0'\Delta K + \Omega_n' \ln\left(\dfrac{c_0'(1-\Delta K) - \Omega_n'}{c_0'(1+\Delta K) - \Omega_n'}\right)^2}{8 c_0'^2 \Delta K}. \quad (21)$$

Therefore, we need to find c_0' and Ω_n' that satisfy the following equation and inequality:

$$\sin\beta_n = \frac{-\pi + \cos\beta_n c_0' \ln\left|\dfrac{(1-\Delta K)\pi - 4\Delta K c_0' \cos\beta_n}{(1+\Delta K)\pi - 4\Delta K c_0' \cos\beta_n}\right|^2}{2\pi c_0'}, \quad (22)$$

$$\frac{(1-\Delta K)\pi}{4\Delta K \cos\beta_n} < c_0' < \frac{(1+\Delta K)\pi}{4\Delta K \cos\beta_n}. \quad (23)$$

Figures 5(a) and 5(b) show critical c_0 values, c_0^*, as a function of the width ΔK of coupling strength inhomogeneity for cases with $H(\theta) = c_0 + \sin(\theta + \beta_1)$. The curves represent numerically obtained c_0^* from Eqs. (16) and (17) or Eqs. (22) and (23). Symbols are for the critical values obtained from simulations. Because of the size effect, it is difficult to determine the critical points by simulations with one value of N. But the size $N=1600$ is large enough to represent well the cases with larger system sizes except near critical points. It still gives small order parameters near critical points. We determine the critical c_0 by the points where time-averaged order parameter becomes less than 0.2. We choose 0.2 as a criterion, because values around this value go to zero as we increase the system size for large values of ΔK (simulations not shown). Such values depend on ΔK and decrease as ΔK decreases, but using 0.2 for all ΔK does not change the result significantly, since c_0^* increases greatly as ΔK decreases. We search for the critical points around theoretically obtained critical c_0 values on the curves with 0.05 intervals. We average the values over states from simulations with ten different configurations. The theoretically obtained curves fit well with the simulation results.

Figure 5(c) shows the theoretically obtained c_0^* for cases without noise as a function of β_1 for several ΔK. The curves for critical values are nonmonotonic in β_1 and the minimum point moves toward $\beta_1 = -\pi/2$ as ΔK increases. For large values of ΔK, the critical value decreases monotonically for wide range of β_1. Next, we determine the parameter range for bistability between a perfectly synchronous state and an incoherent state. Note that the system without noise has a stable synchronous state when $H(0)=0$ and is bistable when c_0^* is less than c_0 for which $H(0)=0$. For $H(\theta) = c_0 + \sin(\theta$

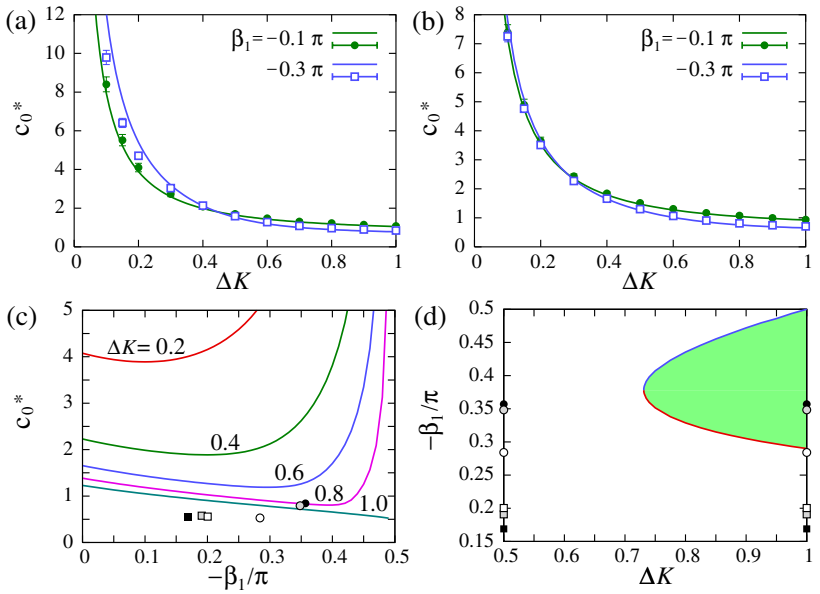

FIG. 5. (Color online) Critical c_0 (c_0^*) and bistable region for cases with $H(\theta)=c_0+\sin(\theta+\beta_1)$. c_0^* with (a) $D=0$ and (b) $D=0.1$ as a function of ΔK. $N=1600$. (c) c_0^* with $D=0$ as a function of β_1. The symbols in (c) denote $(-\beta_1/\pi, c_0)$ for the phase reduction of ML oscillators (see Appendix B). Synaptic (circle) and gap junction (square) coupling cases: $I=45$ (black), $I=50$ (gray), and $I=80$ (white). (d) The curve denotes β_1 with which $c_0^*=-\sin\beta_1$. Bistability between a perfectly synchronous state and an incoherent state occurs in the shaded region where $c_0^*<-\sin\beta_1$ when $D=0$ and $c_0=-\sin\beta_1$. The symbols in (d) denote $-\beta_1/\pi$ for ML oscillators with I as in (c). The symbols and the error bars in (a) and (b) represent the averaged critical c_0 and standard deviation obtained from simulation, respectively. Curves in (a) and (c) are obtained from Eqs. (22) and (23) and those of (b) are from Eqs. (16) and (17). For details, see the text.

$+\beta_1)$, $H(0)=0$ when $c_0=-\sin\beta_1$. So bistability occurs when $H(0)=0$ and $c_0^*<-\sin\beta_1$. In Fig. 5(d), we plot theoretically obtained β_1 values that satisfy the equality $c_0^*=-\sin\beta_1$, as we change ΔK (curves). They exist only for $\Delta K>0.731$, and because of the nonmonotonicity shown in Fig. 5(c), there are two values for each ΔK. The condition $c_0^*<-\sin\beta_1$ is satisfied for the parameter range between the two values (shaded region). The bistability occurs in this parameter region. If $H(0)$ is nonzero, then we cannot, in general, guarantee the existence of a synchronous (or highly coherent) state. However, since $H'(0)>0$, it follows that (i) for $H(0)$ near zero, there remain near synchronous solutions and (ii) they are stable (Theorem 3.1 of Ref. [23]). Thus, we can see the bistability between a coherent state and an incoherent state if $c_0>c_0^*$ and c_0 is close to the one that gives $H(0)=0$.

These results explain the behavior of the ML oscillators described in Sec. II. We plot the $(-\beta_1/\pi, c_0)$ of the phase reduction (see Appendix B) as symbols in Fig. 5(c). Only for the two cases (synaptic coupling with $I=45$ and $I=50$) with which c_0 is above the curve for c_0^* when $\Delta K=1.0$ does the system show incoherent behavior. For these two cases, $H(0)$ is close to zero and thus the system can also exhibit synchronous behavior. For other cases, c_0 is less than c_0^* with all the values of ΔK considered; thus, the system shows coherent behavior. Figure 5(d) also shows this. The coupling functions of ML oscillators can be approximated by $H(\theta)=\sin\beta_1+\sin(\theta+\beta_1)$, where β_1 is from the original H functions (Appendix B), and we plot $-\beta_1/\pi$ for ML oscillators with $\Delta K=0.5$ and $\Delta K=1.0$. The points only for the two cases (synaptic coupling with $I=45$ and $I=50$) with large ΔK are in the bistability region and thus the system can exhibit the bistability with those conditions.

V. SUMMARY AND CONCLUSIONS

In summary, we have investigated the effects of coupling strength inhomogeneity on the synchronization of oscillators. Using phase-reduced models, we have found that inhomogeneity in the total sum of coupling strength to an oscillator can stabilize incoherent states. The mean value of coupling function over one period and the degree of inhomogeneity are the main factors affecting the dynamics of the system. Because they cause effective frequency differences, larger values of either one usually lead to the stabilization of incoherent states. We have analyzed the system using population density method and found the critical point at which an incoherent state becomes stable. We have also found that the system can show bistability between coherent and incoherent states. It is caused by the desynchronization due to the coupling strength inhomogeneity near the parameter range where coherent states are locally stable.

This work may be related to other papers showing that the inhomogeneity in the number of inputs can induce incoherent states [11] or make synchronization harder to achieve [12] in coupled oscillators on networks. This work also seems to be consistent with the fact that weighing the coupling term by the inverse of the number of inputs, which in effect removes the inhomogeneity, can enhance the synchronization [13,14].

ACKNOWLEDGMENT

This work was supported by National Science Foundation Grant No. DMS05135.

APPENDIX A: DETAILS OF THE MORRIS-LECAR MODEL

The functions $m_\infty(V)$, $w_\infty(V)$, and $\tau_w(V)$ in Eq. (1) are defined as follows:

$$m_\infty(V) = 0.5\{1 + \tanh[(V - V_1)/V_2]\},$$

$$w_\infty(V) = 0.5\{1 + \tanh[(V - V_3)/V_4]\},$$

$$\tau_w(V) = 1/\cosh[(V - V_3)/(2V_4)].$$

We use parameter values $E_l = -60$ mV, $E_K = -84$ mV, $E_{Ca} = 120$ mV, $\bar{g}_l = 2$ mS/cm^2, $\bar{g}_K = 8$ mS/cm^2, $\bar{g}_{Ca} = 4$ mS/cm^2, $C = 20$ μF/cm^2, $V_1 = -1.2$ mV, $V_2 = 18$ mV, $V_3 = 12$ mV, $V_4 = 17.4$ mV, and $\phi = 1/15$.

The synaptic gating s_j of Eq. (2) satisfies

$$ds_j/dt = \alpha k(V_j)(1 - s_j) - s_j/\tau_s,$$

$$k(V) = 1/\{1 + \exp[-(V - V_t)/V_s]\}.$$

The values of the parameters are $E_{syn} = 120$ mV, $V_t = 20$ mV, $V_s = 2$ mV, $\alpha = 1$, and $\tau_s = 4$.

APPENDIX B: PHASE REDUCTION FOR MORRIS-LECAR MODEL

Each coupling function is divided by $|c_1|$ for convenience of comparison with the theory. This does not affect the phase distribution of the system in the absence of noise.

With synaptic coupling, $H_{MLs,I=45}(\theta) = 0.8430 + \sin(\theta - 1.1214) + 0.1458 \sin(2\theta - 3.0500) + \text{h.o.t.}$, $H_{MLs,I=50}(\theta) = 0.7912 + \sin(\theta - 1.0940) + 0.1369 \sin(2\theta - 3.1381) + \text{h.o.t.}$, and $H_{MLs,I=80}(\theta) = 0.5283 + \sin(\theta - 0.8927) + 0.1087 \sin(2\theta + 2.3779) + \text{h.o.t.}$, where "h.o.t." means higher-order terms.

With gap junction coupling, $H_{MLg,I=45}(\theta) = 0.5399 + \sin(\theta - 0.5305) + 0.1291 \sin(2\theta - 2.7025) + \text{h.o.t.}$, $H_{MLg,I=50}(\theta) = 0.5757 + \sin(\theta - 0.5995) + 0.1031 \sin(2\theta - 2.8375) + \text{h.o.t.}$, and $H_{MLg,I=80}(\theta) = 0.5569 + \sin(\theta - 0.6292) + 0.0277 \sin(2\theta + 2.2255) + \text{h.o.t.}$

[1] A. Pikovsky, M. Rosenblum, and J. Kurths, *Synchronization: A Universal Concept in Nonlinear Sciences* (Cambridge University Press, Cambridge, England, 2001).
[2] S. H. Strogatz, *Sync: The Emergence Science of Spontaneous Order* (Hyperion, New York, 2003).
[3] Y. Kuramoto, *Chemical Oscillations, Waves, and Turbulence* (Springer, Berlin, 1984).
[4] S. H. Strogatz, Physica D **143**, 1 (2000).
[5] J. A. Acebrón *et al.*, Rev. Mod. Phys. **77**, 137 (2005).
[6] G. B. Ermentrout and D. Kleinfeld, Neuron **29**, 33 (2001).
[7] S. Boccaletti *et al.*, Phys. Rep. **424**, 175 (2006).
[8] S. H. Strogatz, Nature (London) **410**, 268 (2001).
[9] L. F. Abbott and S. B. Nelson, Nat. Neurosci. **3**, 1178 (2000).
[10] S. Song *et al.*, PLoS Biol. **3**, 0507 (2005).
[11] D. Golomb and D. Hansel, Neural Comput. **12**, 1095 (2000).
[12] T. Nishikawa, A. E. Motter, Y.-C. Lai, and F. C. Hoppensteadt, Phys. Rev. Lett. **91**, 014101 (2003).
[13] A. E. Motter, C. Zhou, and J. Kurths, Europhys. Lett. **69**, 334 (2005); Phys. Rev. E **71**, 016116 (2005).
[14] C. Zhou, A. E. Motter, and J. Kurths, Phys. Rev. Lett. **96**, 034101 (2006).
[15] M. Denker, M. Timme, M. Diesmann, F. Wolf, and T. Geisel, Phys. Rev. Lett. **92**, 074103 (2004).
[16] J. G. Restrepo, E. Ott, and B. R. Hunt, Phys. Rev. E **71**, 036151 (2005); Chaos **16**, 015107 (2005); Phys. Rev. Lett. **96**, 254103 (2006).
[17] Y. L. Maistrenko, B. Lysyansky, C. Hauptmann, O. Burylko, and P. A. Tass, Phys. Rev. E **75**, 066207 (2007).
[18] R. Albert and A.-L. Barabási, Rev. Mod. Phys. **74**, 47 (2002).
[19] C. Morris and H. Lecar, Biophys. J. **35**, 193 (1981).
[20] J. Rinzel and G. B. Ermentrout, in *Methods in Neuronal Modeling*, 2nd ed., edited by C. Koch and I. Segev (MIT Press, Cambridge, MA, 1998).
[21] R. A. FitzHugh, Biophys. J. **1**, 445 (1961).
[22] E. M. Izhikevich, *Dynamical Systems in Neuroscience* (MIT Press, Cambridge, MA, 2007).
[23] G. B. Ermentrout, SIAM J. Appl. Math. **52**, 1665 (1992).
[24] G. B. Ermentrout, in *Tutorials in Mathematical Biosciences I*, edited by A. Borisyuk, G. B. Ermentrout, A. Friedman, and D. Terman (Springer, Berlin, 2005).
[25] N. Kopell and G. B. Ermentrout, in *Handbook of Dynamical Systems*, edited by B. Fiedler (Elsevier Science, Amsterdam, 2002), Vol. 2.
[26] S. Watanabe and S. H. Strogatz, Phys. Rev. Lett. **70**, 2391 (1993).
[27] S. Watanabe and S. H. Strogatz, Physica D **74**, 197 (1994).
[28] S. Kim, S. H. Park, and C. S. Ryu, Phys. Rev. Lett. **79**, 2911 (1997).
[29] M. K. Stephen Yeung and S. H. Strogatz, Phys. Rev. Lett. **82**, 648 (1999).
[30] Y. Kuramoto and D. Battogtokh, Nonlinear Phenom. Complex Syst. (Dordrecht, Neth.) **5**, 380 (2002).
[31] D. M. Abrams and S. H. Strogatz, Phys. Rev. Lett. **93**, 174102 (2004).
[32] D. M. Abrams and S. H. Strogatz, Int. J. Bifurcation Chaos Appl. Sci. Eng. **16**, 21 (2006).
[33] S. H. Strogatz and R. E. Mirollo, J. Stat. Phys. **63**, 613 (1991).
[34] S. H. Strogatz, R. E. Mirollo, and P. C. Matthews, Phys. Rev. Lett. **68**, 2730 (1992).